Food Chemistry: X 18 (2023) 100714

Contents lists available at ScienceDirect

Food Chemistry: X

journal homepage: www.sciencedirect.com/journal/food-chemistry-x

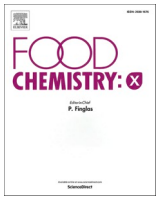

Chitosan/esterified chitin nanofibers nanocomposite films incorporated with rose essential oil: Structure, physicochemical characterization, antioxidant and antibacterial properties

Yingzhu Liu [a,1], Rongxu Liu [b,c,1], Jingbo Shi [a], Rui Zhang [b], Hongjie Tang [b], Cancan Xie [b], Fenghui Wang [b], Jianchun Han [b,c,*], Longwei Jiang [b,*]

[a] College of Horticulture and Landscape Architecture, Northeast Agricultural University, Harbin 150030, China
[b] College of Food Science, Northeast Agricultural University, Harbin 150030, China
[c] Heilongjiang Academy of Green Food Science, Northeast Agricultural University, Harbin 150028, China

ARTICLE INFO

Keywords:
Chitosan
Chitin nanofibers
Active packaging
Essential oil
Physicochemical properties

ABSTRACT

Active films were developed based on chitosan, esterified chitin nanofibers and rose essential oil (REO). The joint effects of chitin nanofibers and REO on structure and physicochemical properties of chitosan film were investigated. Scanning electron microscopy and Fourier transform infrared spectroscopy showed that the chitin nanofibers and REO had significant effects on the morphology and chemical structure of chitosan composite films. The negatively charged esterified chitin nanofibers formed a compact network structure through intermolecular hydrogen bonding and electrostatic interactions with the positively charged chitosan matrix. Chitin nanofibers and REO synergistically enhanced the water resistance, mechanical properties and UV resistance of chitosan-based films, but the addition of REO increased the oxygen permeability. Furthermore, the addition of REO enhanced the inhibition of ABTS and DPPH free radicals and microorganisms by chitosan-based film. Therefore, chitosan/chitin nanofiber-based active films containing REO as food packaging materials can potentially provide protection to extend food shelf life.

1. Introduction

Polymer plastics synthesized from petroleum are the most widely and commonly applied materials in food packaging. Nevertheless, serious environmental pollution has resulted from the use of plastics, and these materials are not degradable (Zhang et al., 2020). In addition, several studies have reported the toxic effects of plastics in human cell lines (Danopoulos, Twiddy, West, & Rotchell, 2022), marine organisms (Han et al., 2022), and various tissues and organs (Yin et al., 2021). Worryingly, scientists have recently found the presence of microplastics in human breast milk (Ragusa et al., 2022). Therefore, packaging research has recently been focused on nontoxic, edible and/or biodegradable packaging materials developed from natural polymers (Wang et al., 2022). Chitosan is an ideal candidate for biopolymer films with excellent film-forming, nontoxic, renewable, biodegradable and biocompatible properties, and is recognized as a safe GRAS grade polymer (Choo, Lin, & Mustapha, 2021). Due to its versatility, chitosan has been used in tissue engineering applications, but also in the field of drug delivery systems, dietary supplements, cosmetics, antimicrobial mouthwashes, plant cultivation and environmental protection processes (Bakshi, Selvakumar, Kadirvelu, & Kumar, 2020). In addition, the presence of hydroxyl and amino functional groups enables many different chemical and enzymatic modifications, which are often used to design and construct systems used for the immobilization and release of therapeutic compounds and to obtain water-soluble chitosan derivatives (Geng et al., 2023). Chitosan is derived from chitin, and the degree of biopolymer deacetylation is greater than 60 %. The worldwide chitin and chitosan market has shown tremendous growth, which has been propelled by increased application. The market volume was projected to be more than 155,000 metric tons by 2022 (Jardine & Sayed, 2018). However, there are many hydrophilic groups in chitosan, and the mechanical, barrier and water resistance properties of chitosan films are insufficient, which limits its application in food packaging (Zhang et al., 2018).

* Corresponding authors at: College of Food Science, Northeast Agricultural University, Harbin 150030, China (J. Han).
E-mail addresses: hanjianchun@hotmail.com (J. Han), jianglw58@163.com (L. Jiang).
[1] These authors contributed equally to this work.

https://doi.org/10.1016/j.fochx.2023.100714
Received 22 March 2023; Received in revised form 7 May 2023; Accepted 15 May 2023
Available online 18 May 2023

One way to overcome these disadvantages is to improve the physicochemical properties of the films by blending chitosan and other bio-based polymer nanomaterials to prepare biocomposites (Tang, Zhang, Zhao, Guo, & Zhang, 2018). In our previous research, cellulose nanocrystals were incorporated into zein films, and the barrier, mechanical and UV resistance properties of the films were significantly enhanced (Jiang, Han, Meng, Xiao, & Zhang, 2021a). Chitin, the second largest natural polymer after cellulose, consists of 2-acetamino-2-deoxy-D-glucose with β (1–4) bonds and is found primarily in the exoskeletons of crustaceans (Jafari, Pirouzifard, Khaledabad, & Almasi, 2016). Chitin nanofibers are extracted from chitin by various mechanical or chemical methods, and they exhibit diameters of<100 nm, which has the characteristics of good biocompatibility, large specific surface areas, small sizes, and high mechanical strengths (Ding, Deng, Du, Shi, & Wang, 2014). The fascinating properties of chitin nanofibers have attracted considerable attention from researchers, and many studies have shown that chitin nanofibers have the ability to enhance the performance of biopolymer films (Jafari, Pirouzifard, Khaledabad, & Almasi, 2016; Pasquier et al., 2022). Many polymeric materials with various applications in industry, medicine and pharmacy have been obtained by modification of the chitin (Bakshi et al., 2020). Wang et al. (2018) previously obtained chitin nanofibers via solvent-free esterification with maleic anhydride and chitin combined with ultrasonication. The surfaces of the esterified chitin nanofibers were negatively charged due to the introduction of carboxylate (–COO-) groups. Prior studies have shown that polymers with opposite charges form compact polymer networks via electrostatic interactions and hydrogen bonding, thus enhancing the film performance (Chen et al., 2023; Leite, Moreira, Mattoso, & Bras, 2021). Inspired by previous studies, the film matrix formed by the chemically active positively charged amino group ($-NH_2$) in the flexible chain of chitosan and the negatively esterified chitin nanofibers has great potential for use in packaging materials.

In recent years, many natural biomolecules have been widely used to enhance the activities and functionalities of biocomposite polymer films, especially hydrophobic essential oils (Li et al., 2021a). Wang et al. (2021) prepared starch-based films containing bamboo leaf oil through solution casting, and the starch films showed significantly enhanced flexibility, water resistance, UV resistance and antibacterial properties. The rose is a woody perennial flowering plant of the Rosa genus in Rosaceae. Roses are commonly used in traditional cosmetics, medicines, foods and textiles because they are rich in bioactive compounds: these include the petals, pseudo-fruits (apparent fruits) and real fruits (nuts, seeds), which appear in vitamins (mainly C), polyphenolic compounds, carotenoids, fatty acids belonging to the valuable families: n-6 (linoleic, arachidonic), n-3 (linolenic), n-9 (oleic acid), minerals, pectins, carbohydrates, including sugars and fibres, organic acids (citric, malic), essential oils, amino acids and waxes (Cendrowski, Scibisz, Kieliszek, Kolniak-Ostek, & Mitek, 2017; Cendrowski, Scibisz, Mitek, & Kieliszek, 2018; Cendrowski, Ścibisz, Mitek, Kieliszek, & Kolniak-Ostek, 2017). Rose essential oil (REO) contains a variety of active ingredients, including citronellol, geraniol, and eugenol (Maciąg & Kalemba. 2015), which are potential bioactive compounds that can be incorporated into polymer matrices to form active packaging due to their antimicrobial and antioxidant capacities and abilities to improve the food flavor; in addition to their role in improving the physical properties of films. However, it was found that essential oil droplet can deform and penetrate into the film matrix and cause structural discontinuity of the polymer film, which leads to increased flexibility and decreased tensile strength (Li, Tang, & He, 2021; Wang, et al., 2021). The emulsification of surfactants can be used to effectively incorporate essential oils into emulsions, which is a potential tool for improving physicochemical properties and compatibility of essential oils with film matrix (Chu et al., 2020). In this study, we sought to use negatively charged esterified chitin nanofibers and positively charged chitosan to construct a dense film matrix via electrostatic interactions and hydrogen bonding to resist the adverse effects of essential oils on the mechanical strength of the film. Furthermore, there has been no research specifically focused on the construction of bioactive films containing chitosan, chitin nanofibers and REO. There are still significant gaps in the insight into the properties and structure of chitosan/chitin nanofibers/REO films.

Hence, the objectives of current study were to develop chitin nanofibers reinforced chitosan films incorporating REO as an active filler, to investigate the effects of REO at different concentrations on the structure of the composite films, and to characterize the barrier, mechanical and optical properties and the water solubility of the biofilms. The micromorphology, compatibility, structure and thermal properties of the films were investigated through scanning electron microscopy, Fourier transform infrared spectroscopy, thermogravimetric analyses, and X-ray diffraction measurements. The antibacterial and antioxidant capacities of the biocomposite films were also investigated. Great attention has been given to the safety and quality of food products, which has led to innovations in the food packaging industry. In view of the diversity of products in the active food packaging industry, this study provides theoretical support for the development of nanocomposite films containing essential oils, in order to stimulate the development of new packaging products in industry.

2. Materials and methods

2.1. Materials

Chitosan (deacetylation degree of 95%) and 2,2′-azino-bis (3-ethylbenzothiazoline-6-sulfonic acid) diammonium salt (ABTS) were purchased from Macklin Biochemical Co., Ltd. (Shanghai, China). Chitin was obtained from Aladdin Chemical Co., Ltd. (Shanghai, China). REO was obtained from Shanghai Yuanye Biotechnology Co., Ltd. (Shanghai, China). *S. aureus* (ATCC6538) and *E. coli* (ATCC25922) were purchased from the Beijing Microbiological Culture Collection Center (Beijing, China). 2,2-Diphenyl-1-picrylhydrazyl (DPPH) was obtained from Solarbio Technology Co., Ltd. (Beijing, China). All other chemicals were analytical grade.

2.2. Development of chitin nanofibers

Esterified chitin nanofibers were prepared following a previous method (Wang et al., 2018). Maleic anhydride (25 g) and chitin powder (5 g) were mixed and then reacted at 120℃ (3 h). The esterification process does not require stirring and solvent, and has the advantages of environmental friendliness, low cost and easy purification. Afterward, the esterification product was washed with absolute ethanol (200 mL) and then water until the filtrate pH reached 7.0. Then, NaOH (1.0 M) was added to the solution to raise the pH to 11.0 and the mixture was rinsed with water until the pH of the suspension reached 7.8. Finally, purified water was added into the suspension until the concentration of the chitin suspension was 1 wt%. A 30 g suspension of esterified chitin was treated with an ultrasound generator (SCIENTZ-11D, China Xinzhi Biotechnology Co., LTD.). The treatment conditions were 500 W, 0.5/4 s on/off pulses, and 45 min, and uniform chitin nanofibers were obtained.

2.3. Preparation of films

The biofilms were prepared according to the method of Wang et al. (2023) with some modifications. Chitosan (2.4 g) was dissolved in a 2% (v/v) acetic acid solution (120 mL) with continuous stirring for 1 h at 50℃. Then, a chitin nanofiber suspension containing 5 wt% chitin nanofibers (based on chitosan) was added to the chitosan solution with stirring for 0.5 h and then ultrasonicated for 5 min. The solution was cooled to room temperature, and 1% (v/v) Tween 80 emulsifier was added to the film-forming solutions with stirring for 10 min. Finally, different contents of REO (0.5, 1, and 2%, v/v) were added and then homogenized at 10000 rpm for 10 min with a high-speed dispersion homogenizer (AD300L-H, Shanghai ONI Instrument Co., Ltd., China).

After degassing, the film-forming solution was poured into a mold (18 × 26 cm). The chitosan-based film was peeled off from the mold after drying, and the film was stored for 48 h at 75% relative humidity before testing. The chitosan film and chitosan film with chitin nanofibers were named CS and CN, respectively, while the films containing different REO concentrations (0.5, 1, and 2%) were denoted as CN0.5 %REO, CN1% REO and CN2%REO.

2.4. Structural characterization of the films

An X-ray diffractometer (D8 Advance, Bruker, Karlsruhe, Germany) with Cu Kα radiation and a scan range of $2\theta = 5^{\circ}$ and 50° was used to obtain X-ray diffraction (XRD) patterns. Fourier transform infrared (FT-IR) spectra of the samples were obtained in the range of 4000–400 cm^{-1} by a spectrometer (Nicolet is 50, Thermo Fisher Scientific, USA). The morphology of the films was observed by scanning electron microscope (SEM, Hitachi S-3400 N, Japan). A thermogravimetric analyzer (SDT 650, TA, USA) was used for TGA tests to monitor the thermal characteristics of the films at a rate of 10 ℃/min under N_2 (100 mL/min) from 30℃ to 800℃.

2.5. Thickness, moisture content (MC) and water solubility (WS)

A thickness meter (NO:7301, Japan Mitutoyo Co., LTD, Japan) was used to measure the thickness of the film. The MC of the film sample was measured as described in our previous study (Jiang et al., 2022a). The sample was dried (105℃, 24 h), and the MC was determined from the reduced weight of the film as a percentage of its initial weight. The WS of the samples was measured as described in our previous study (Jiang et al., 2022b). The film was divided into 1 × 6 cm pieces and stirred in distilled water for 6 h at 150 rpm. The ratio of the reduced weight to the initial weight of the film was taken as WS.

2.6. Optical properties of films

The transmittance of the sample was tested using a UV–vis spectrophotometer (UV-2660, Shimadzu, Japan) from 200 to 800 nm. Photos of the films placed on white paper with the university's emblem were taken with a digital camera. The color parameters (a, b and L^*) of the sample were tested with a colorimeter (CR-20, Konica Minolta, Tokyo, Japan). The total color difference (ΔE) of each film was calculated as follows:

$$\Delta E = \sqrt[2]{\Delta L^2 + \Delta a^2 + \Delta b^2} \quad (1)$$

where ΔL, Δa, and Δb are the differences for each color value of the film sample relative to the standard plate, respectively.

2.7. Mechanical properties

The film samples were sliced into 1 × 6 cm strips. A universal testing machine (Byes-1001, Bangyi Precision Measuring Instrument Co., Ltd., China) equipped with a 500 N sensor was used to measure the elongation at break (EAB) and tensile strength (TS) of film samples with a tensile speed of 1 cm/min.

2.8. Water vapor permeability (WVP)

WVP was measured as described previously and based on ASTM standard method E96-80 (Jiang, Jia, Han, Meng, Xiao, & Bai, 2021b). The test cup, which had an inner diameter of 6 cm, an outside diameter of 9 cm, and a depth of 2.2 cm, contained anhydrous $CaCl_2$ and was sealed with various films. The test cup was stored in a desiccator with 95% RH at room temperature. The test cup was weighed every 2 h.

2.9. Oxygen permeability (OP)

The OP of the sample was tested following a previous study (Li et al., 2021b). Tubes containing 1 mL of linoleic acid were sealed with the film samples and then stored for 7 days in darkness at room temperature, and their weights were checked every 24 h. The oxygen transmittance was determined by the weight increase of the linoleic acid. The OP was calculated with Eq. (2):

$$OP = \frac{\Delta M}{S \times T} \quad (2)$$

where S is the area of film permeation (m^2), ΔM is the weight change of the linoleic acid (g), and T is the test time (d).

2.10. Water contact angle (WCA)

WCA of the films was tested according to our previous method (Wang et al., 2023). A PD-200 contact angle analyzer (Attension Theta, Biolin Scientific, Finland) was used to test the WCA of the samples. Distilled water drops (5 μL) were deposited on the surface of the sample, and the process was recorded. Six different sample positions were selected for testing.

2.11. Swelling ratio (SR)

The SR of the sample was tested according to the method of Zhang et al. (2018). The film was cut into 2 × 2 cm pieces, and the weights was recorded as W_0. Then, the film was immersed in 30 mL phosphate buffer saline for 30 min at room temperature. The sample was removed, and the surface moisture was wiped off with filter paper, and the weight was recorded as W_1. The SR was calculated as follows:

$$SR(\%) = \frac{W_1 - W_0}{W_0} \times 100 \quad (3)$$

2.12. Antioxidant capacity of films

The DPPH radical scavenging activity and the ABTS radical cation scavenging activity of films were determined by the method of Jiang et al. (2021b). The film (20 mg) was put into a DPPH ethanol solution (0.2 mM, 4 mL) in a dark tube at room temperature for 30 min. Then, the absorbance was measured at 517 nm. The film (40 mg) was put into 4 mL ABTS + solution for 6 min, and the absorbance was tested at 734 nm. The antioxidant activity of the samples was determined as follows:

$$\text{Antioxidant activity}\ (\%) = \frac{A_0 - A_1}{A_1} \times 100 \quad (4)$$

where A_0 and A_1 are the absorbances of the control with no film and the test film, respectively.

2.13. Antimicrobial activity of films

The antimicrobial activity of the samples was determined based on the method of Wang et al. (2023). Briefly, *S. aureus* and *E. coli* were inoculated in nutrient broth for activation, and then the film sample was cut into discs (diameter 10 mm). Microbial suspensions (100 μL) were inoculated in Luria-Bertani agar plates. The films were placed into a culture medium coated with *S. aureus* and *E. coli*, incubated in a 37℃ incubator for 24 h, and then the inhibition size was determined.

2.14. Statistical analysis

All experiments were repeated at least three times. All data were subjected to one-way analysis of variance and Duncan's multiple comparison test (significance level $p < 0.05$) to verify whether there were significant differences among the means. Experimental data are

expressed as the mean ± standard deviation (SD).

3. Results and discussion

3.1. Structural characterization of the films

The crystalline structure of the biopolymer films was analyzed by XRD. Fig. 1A displays the XRD patterns of the different samples. For chitin nanofibers, there were 2 main diffraction peaks at 2θ = 9.4 and 19.4°, indicating their crystalline nature, which was consistent with the results of a previous study (Wang et al., 2018). Chitosan films presented four main diffraction peaks at approximately 2θ = 8.3, 11.4, 18.3 and 23.0° with a semicrystalline state (Jiang et al., 2021c). A previous study reported that chitosan comes in three forms: anhydrous crystalline, hydrated crystalline and amorphous chitosan (Shahzadi et al., 2016). The diffraction peak for CS at 2θ = 23.0° showed a crystalline region; this is a typical fingerprint for ordinary chitosan films and is attributed to the regular crystalline lattices of chitosan and hydrated crystals (Zhang, et al., 2018). After the chitin nanofibers were added, the chitosan film still showed four characteristic peaks. However, the intensity of the CN diffraction peak at approximately 2θ = 18.3° was stronger relative to those of the chitin nanofibers that enhanced the crystallinity of the film, which was conducive to enhancing the tensile strength and barrier properties of the biopolymer film (Jiang et al., 2022a). When REO was added to the CN, there were still four peaks in the XRD diffraction patterns. This indicated that addition of the essential oil did not change the crystal structure of the biofilm, and REO showed good biocompatibility with the film matrix. It is worth noting that the crystallinity of the film did not change obviously when the REO contents were 0.5% and 1%, while the crystallinity of the film increased obviously when the content of REO was 2%; this may have been related to interactions between the REO and the film matrix. One possibility was that at lower concentrations, the essential oil was partially volatilized and therefore had less effect on the crystallinity. Another possibility was that a high concentration of the essential oil interacted with the film matrix, reduced phase separation and aided the plasticization process (de Souza, dos Santos, da Silva Torin, & dos Santos Rosa, 2020). Zhang et al. (2018) also reported that the addition of *Perilla frutescens* (L.) Britt. essential oil enhanced the crystallinity of a chitosan film. These diffraction patterns indicate that REO- and chitin nanofiber-reinforced chitosan films formed denser crystalline domains than pure CS.

FT-IR was used to monitor intermolecular interactions among the chitin nanofibers, REO, and chitosan that are related to the physicochemical properties of the biofilms. FT-IR spectra of the chitin nanofibers, REO and chitosan-based film are displayed in Fig. 1B. Strong and broad bands were found between 3000 and 3500 cm^{-1} and indicated –OH stretching vibrations. For REO, the absorption bond at 2956 cm^{-1} was due to C═C-C ring vibrations of the volatile compounds in the essential oil (Cebi, Arici, & Sagdic, 2021). The strong absorption bands at 1743, 1369 and 1216 cm^{-1} corresponded to the C═C, C—H and C—O stretching vibrations, respectively (Cebi, 2021). For the esterified chitin nanofibers, the amide bands at 1662 cm^{-1} and the amide II band at 1565 cm^{-1} were characteristic of α-chitin. It is worth noting that there was an absorption peak at 1724 cm^{-1} in the FTIR spectrum of the chitin nanofibers, which was attributed to the − COO– of the maleate moiety (Wang et al., 2018). These results confirmed that the maleate groups were successfully grafted onto the chitin nanofibers. Wang et al. (2018) also found a similar phenomenon in a previous study. When chitin nanofibers were added to CS, the –OH peak at 3236 cm^{-1} for CS moved to 3218 cm^{-1} for CN, suggesting that the chitin nanofibers had formed intermolecular hydrogen bonds with the chitosan matrix (Jiang et al., 2021b). Moreover, CS and CN showed similar FTIR spectra, indicating that incorporation of the chitin nanofibers did not change the chemical structure of chitosan; this confirmed that the chitin nanofibers and chitosan were biocompatible. The formation of hydrogen bonds was beneficial to improve the physical performance of the biopolymer film. With the addition of REO, the peak of the –OH group of CN at 3218 cm^{-1} gradually moved to smaller wavenumbers, 3189, 3177 and 3167 cm^{-1} for CN0.5 %REO, CN1%REO and CN2%REO, respectively. These results showed that intermolecular hydrogen bonds were formed between the chitosan, chitin nanofibers and REO. It is noteworthy that new absorption peaks appeared at 1743, 1369 and 1216 cm^{-1} after addition of the essential oil; these originally belonged to REO, and the intensities of the peaks increased with increasing amounts of REO. This was due to the

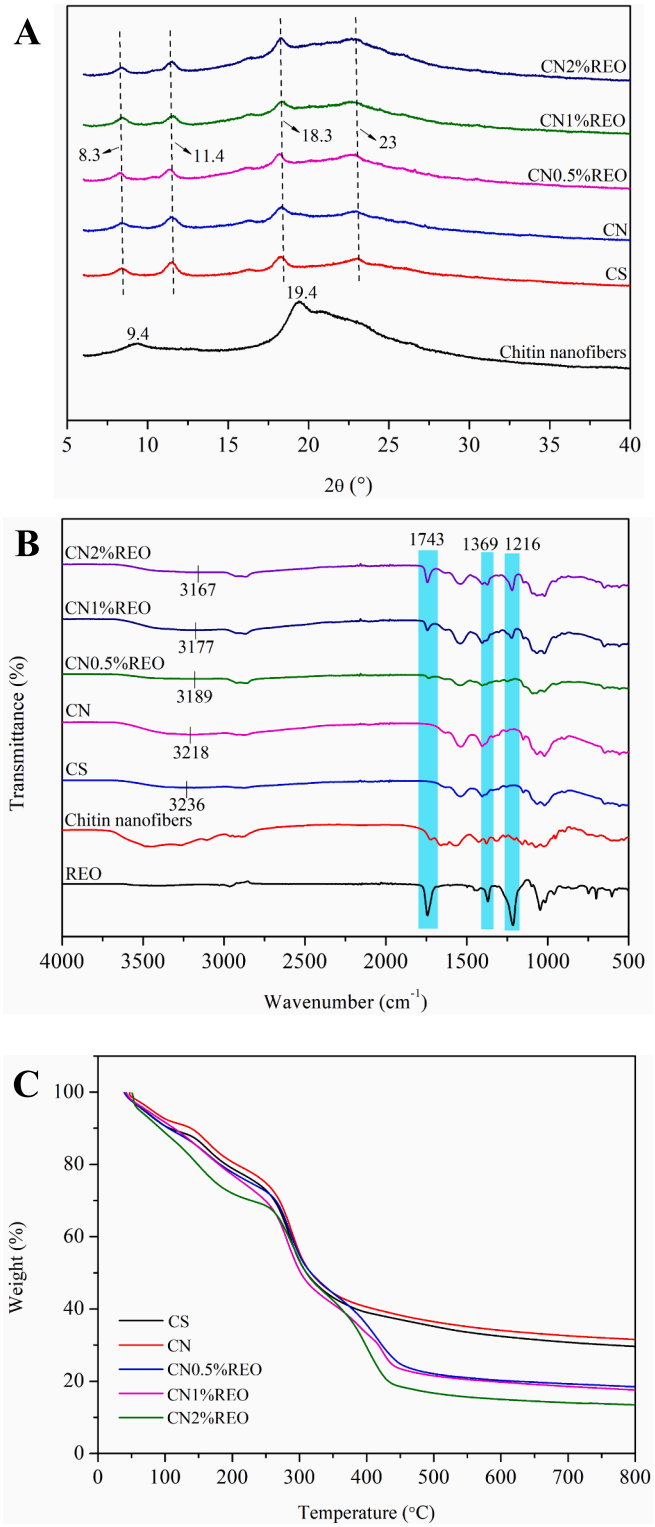

Fig. 1. XRD patterns (A), FT-IR spectra (B) and TGA profiles (C) of the samples.

enrichment of REO in the film, and successful incorporation of the essential oil could improve the antibacterial and antioxidant properties of the active packaging. Saricaoglu and Turhan (2020) also reported a similar phenomenon when clove essential oil was added to a polymer film. A new peak was found at 1743 cm^{-1} in the CN-REO films, indicating increased interactions between the essential oil and the film matrix with increasing REO concentration (Flórez, Cazón, & Vázquez, 2022). The C═O tensile vibration in the ester structure of fatty acids was the cause of this band, which was the unique band of oil (Flórez, Cazón, & Vázquez, 2022). In addition, due to the interaction between the essential oil and the film matrix, the peak strength at 1216 and 1743 cm^{-1} attributed to the amide-III and amide I bands for the CS-based blend film increased (Pan, et al., 2023). It can be determined that the addition of REO and chitin nanofibers to CS modified the spectrum of CS. All of these changes may be related to the possible molecular compatibility and intermolecular interaction between the functional groups of the essential oil and the $–NH_2$/–OH groups of the film matrix.

Fig. 1C displays the TGA curves of film samples. The chitosan-based films with different contents of REO exhibited 3 main weight loss stages. In the 1st stage (40-200℃), all of the films lost approximately 20–30% of the original weight, and this was attributed to the loss of free and bound water, and other volatile ingredients absorbed in the film (Li et al., 2021a). The 2nd weight loss stage occurred at approximately 40–50% within the degradation temperature range from 200 to 400℃, corresponding to the degradation of polymer chains and residual aromatic compounds of the essential oil (Zhang, et al., 2018). The thermal degradation in the 3rd stage (above 400℃) involved decomposition of the cross-linked structure and degradation of the remaining film matrix (Alizadeh-Sani et al., 2020). Obviously, when the chitin nanofibers were added to the chitosan, the TGA curve for CN shifted to higher temperatures, and more residual matter was retained at 800℃, suggesting that the chitin nanofibers enhanced the thermal stability of the CS; this also indicated that there were strong interactions formed between chitin nanofibers and the chitosan matrix. Huq et al. (2012) reported a similar phenomenon: when cellulose nanocrystals were added to alginate-based films, the thermal stability was improved. In addition, films with REO have greater thermal degradation and less dry matter retained at 800℃ than CS and CN, which may have been due to the volatile nature of the essential oil as well as plasticization in which the REO might dispute the interactions among the polymer chains of the composite film networks (Li et al., 2021a).

To gain further insight into the microstructure of the chitosan composite films, they were analyzed by SEM. Fig. 2 and Fig. S1 show the microstructure of biopolymer films at different magnifications. The microscopic surface of CS was dense and smooth, and the cross-sectional structure was uniform and less rough, which was consistent with the results observed in our previous study (Jiang et al., 2021c). After addition of the chitin nanofibers, the surface morphology of CN was still compact and smooth, while the roughness of the cross-section morphology of CN was reduced, and the microstructure became dense and continuous, which confirmed the compatibility of chitosan and the chitin nanofibers. The compact microstructure was conducive to enhanced the physical properties of the biopolymer films (Jiang et al., 2022a). However, the surface roughness of the films increased after the incorporation of REO. A similar microstructure was reported by Zhang et al. (2018), who added *Perilla frutescens* (L.) Britt. essential oil to CS and increased the surface roughness of the chitosan-based film. After adding different levels of REO into the chitosan-based film, the cross-sectional microstructure of the film changed greatly and became heterogeneous. As the amount of essential oil was increased, the number of bubble-like oil droplets also increased, and they were closely bound to the polysaccharide matrix. The porous structure of the cross-sections became increasingly obvious (Fig. 2D and E). This might be due to the traction forces induced by the chitosan network during the evaporation of volatile oil in the cross-section of films (Hafsa et al., 2016). In addition, a microporous structure like that of a “sponge” might improve the flexibility of the film, and we speculate that larger pores may increase the gas permeability of the film.

To further explore the mechanism for the interactions between the components in the film matrix, a Zetasizer Nano-ZS90 (Malvern, UK) was used to determine the zeta potential of the film-forming solution. The zeta potential of the chitin nanofibers was -44.58 ± 1.69 mV, and the mean particle size was 210.9 ± 5.1 nm. These results showed that the maleate groups were successfully grafted onto the chitin nanofibers and that the chitin nanofibers were negatively charged. Modification of the polymers improved a number of the physicochemical and processing properties; in many cases, this is more economical than synthesizing new monomers and polymers. Polymer modifications are generally divided into two types: chemical modification and physical modification. Chitin nanofibers were successfully prepared from a commercially available chitin powder via esterification modification and subsequent ultrasound treatment. Since no solvents or stirring were needed for the esterification reaction, it offers the advantages of low cost, environmental friendliness, and easy purification. The chitosan solution had a zeta potential of 44.25 ± 1.42 mV, which was caused by the positive charges in chitosan resulting from protonation of the NH_2 groups (Wang et al., 2023). It should be noted that when 5 wt% chitin nanofibers were added, the zeta potential decreased to 16.23 ± 1.65 mV. This was due to electrostatic attractions between the negatively charged chitin nanofibers and positively charged chitosan, which resulted in partial charge neutralization (Wang et al., 2023). Therefore, the mechanism for the internal interactions of the films can be inferred from these research results. As shown in Fig. 3, the chitin nanofibers formed a dense network structure with the film matrix through electrostatic interactions and intermolecular hydrogen bonding. Moreover, the esterified chitin nanofibers also acted as crosslinking agents after heating and established crosslinked networks in the polymer matrix of the film (Jiang et al., 2022b). The REO was coated with Tween 80, the hydrophilic group-hydrophilic head and hydrophobic tail formed stable micelles in the film, and the REO wrapped the film so that no phase separation occurred during preparation of the composite film. Meanwhile, the hydrophilic head groups and some unsaponified components were bonded to polymer molecules by hydrogen bonds (Wang, et al., 2022).

3.2. Thickness, MC and WS

Table S1 displays the thickness, MC and WS of the films. CS had the lowest mean thickness of 0.053 ± 0.003 mm. After the incorporation of chitin nanofibers and REO, the film thickness was significantly increased ($p < 0.05$), which was associated with increased dry residue from the films, and REO droplets filled the network of the film and acted as film fillers (Wang, et al., 2022). CS had the highest MC of $23.16 \pm 0.69\%$. The MC of the composite biofilms decreased significantly after adding chitin nanofibers and REO ($p < 0.05$). The addition of chitin nanofibers and essential oils increased the hydrophobicity and reduced the humidity sensitivity of the chitosan-based films. In addition, many intermolecular hydrogen bonds were formed among the REO, chitin nanofibers and chitosan, which weakened the interactions between water molecules and the film matrix (Jiang, et al., 2022b). Previous studies also showed that the addition of essential oils reduced the water contents of biopolymer films (Li et al., 2021b; Wang, et al., 2021; Zhang, et al., 2018). Solubility is one of the important features of food packaging materials. When packaging food with a high MC, the packaging materials must have low WS. CS had the highest WS of $14.47 \pm 0.17\%$. After incorporation of the chitin nanofibers and the essential oil, the WS of the composite films decreased obviously ($p < 0.05$). The reason was that both chitin nanofibers and REO were insoluble in water, and their combination with chitosan reduced the solubility of the film. Moreover, the intermolecular interactions among the film matrix, REO and the chitin nanofibers limited the solubility of the film in water (Jiang, et al., 2022b).

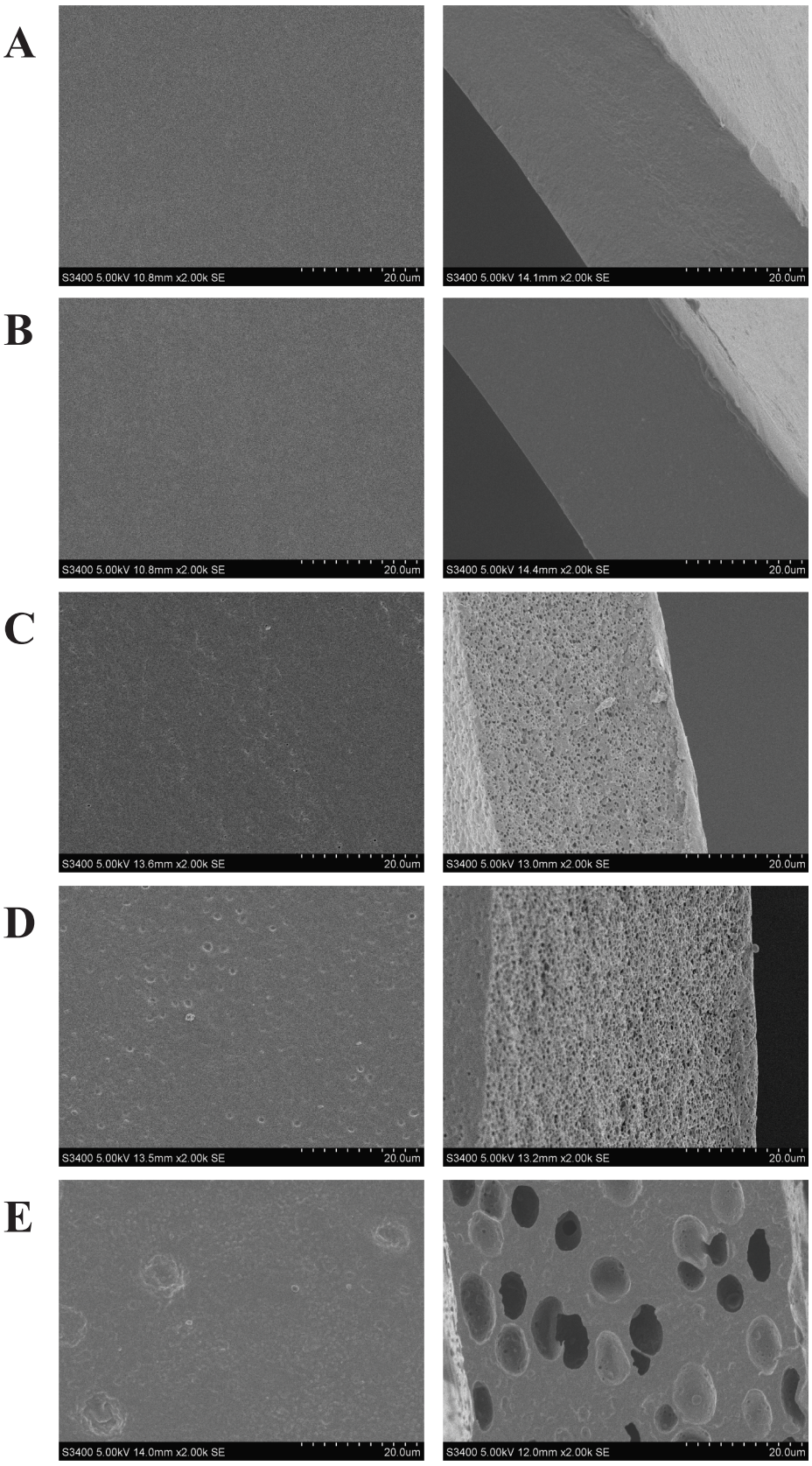

Fig. 2. The surface and cross-section morphology of CS (A), CN (B), CN0.5 %REO (C), CN1%REO (D), CN2%REO (E).

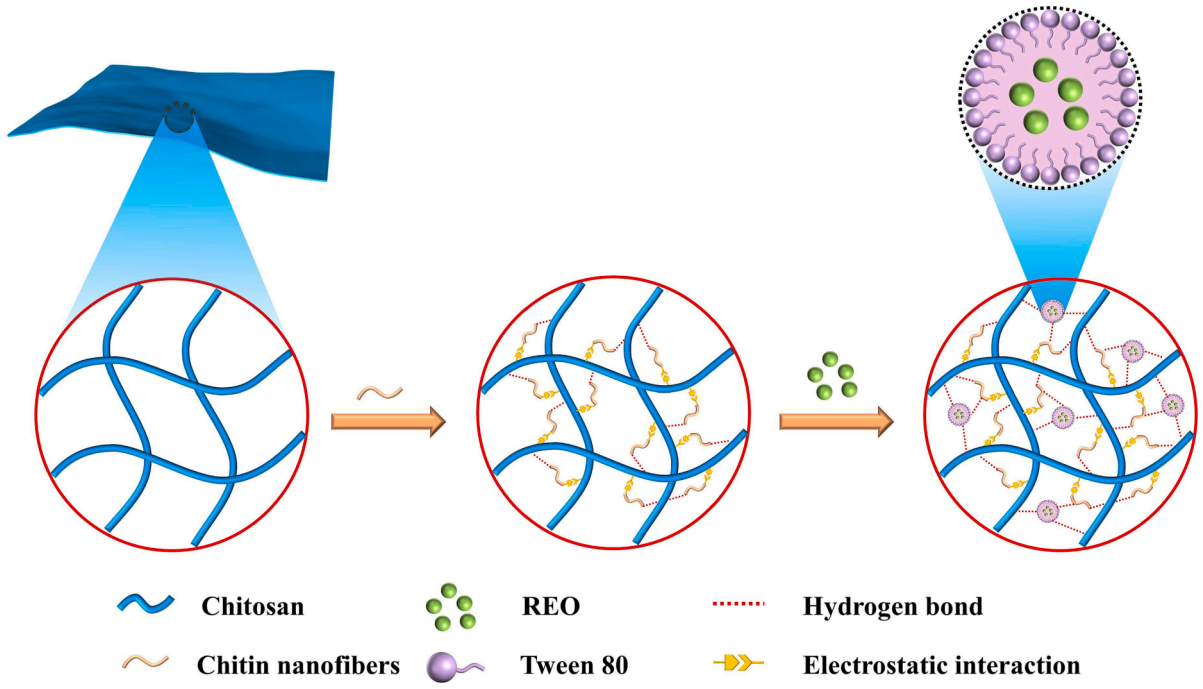

Fig. 3. The schematic diagram of the internal interaction of the film.

3.3. Optical properties of films

Fig. 4 presents the physical appearances of the chitosan-based films. CS presented the highest transparency on printer paper. The transparency of CN was slightly reduced by the addition of chitin nanofibers. As the amount of REO increased, the transparency of chitosan-based films decreased significantly, and the yellowness of the films increased. In addition to the color darkening caused by the addition of REO, the observed results might be related to the light scattering, reflection and coalescence effects caused by large REO molecules distributed throughout the film matrix. Basically, oil droplets localized in the film matrix increased the opacity, more likely due to their light scattering action (Li et al., 2021a). Table S1 presents the color parameters (a, b, L^* and ΔE) of the films. The a value indicates greenness to redness, the b value indicates blueness to yellowness, and the L^* value indicates the light–dark intensity (Jiang, et al., 2022b). The incorporation of chitin nanofibers and REO significantly decreased the a and L^* values from 2.75 ± 0.14 to −3.76 ± 0.14 and 88.37 ± 0.36 to 76.50 ± 0.84 ($p < 0.05$), respectively, while the b value increased from −10.88 ± 0.77 to 20.71 ± 1.78, indicating a trend toward darkness and yellowness. The ΔE of the films increased significantly with increasing REO content compared to CN ($p < 0.05$), which showed that REO had a high effect on the color of the films due to its intrinsic yellow color (Li et al., 2021a). The color parameters of the film measured by colorimeter were consistent with observations by the naked eye observation. UV–vis barrier capabilities play an important role in regulating the sensory properties of packaged foods and delaying lipid oxidation (Jiang, et al., 2022b). Fig. 4 displays the light transmittance of film samples. The light transmittance of the films decreased after the chitin nanofibers were added. After the incorporation of REO, the transmittance of chitosan-based films decreased significantly. These results indicate that films containing REO have good light barrier capability, which may be due to the UV radiation absorption ability of phenolic compounds in essential oils (Li et al., 2021b). A previous study found a similar phenomenon when coffee oil was incorporated into corn starch-based film (Wang, et al., 2022). In addition, the REO droplets dispersed in the film to keep out the light path, thus reducing the light transmittance of film. In particular, the transmittance of the films containing REO was almost 0 in the UV region (200–300 nm), indicating that the CN-REO films have excellent anti-UV ability. Therefore, the biocomposite films containing REO have potential application value as UV-sensitive food packaging materials, thus extending the shelf life of food products.

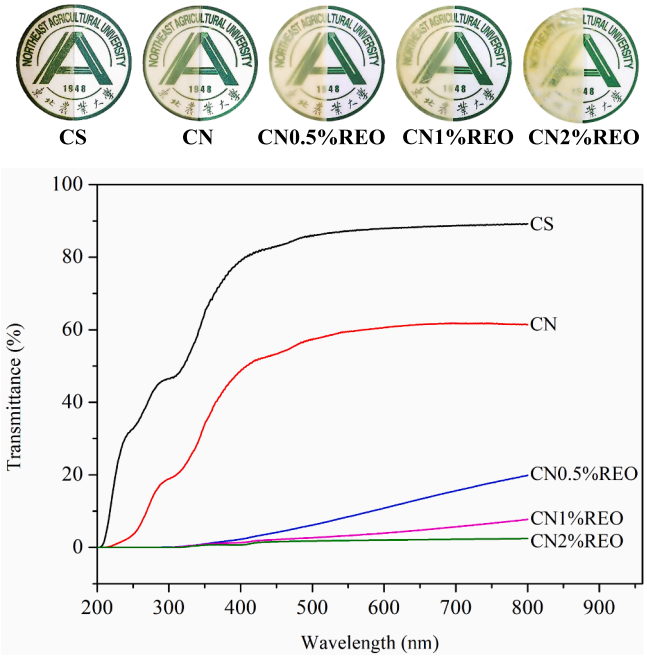

Fig. 4. The physical appearances and UV–vis light transmittance of CS, CN, CN0.5 %REO, CN1%REO and CN2%REO.

3.4. Mechanical properties

The stress–strain curves obtained from tensile measurements of film samples are displayed in Fig. S2, and the mechanical properties (EAB and TS) are displayed in Fig. 5A-B. The addition of chitin nanofibers and

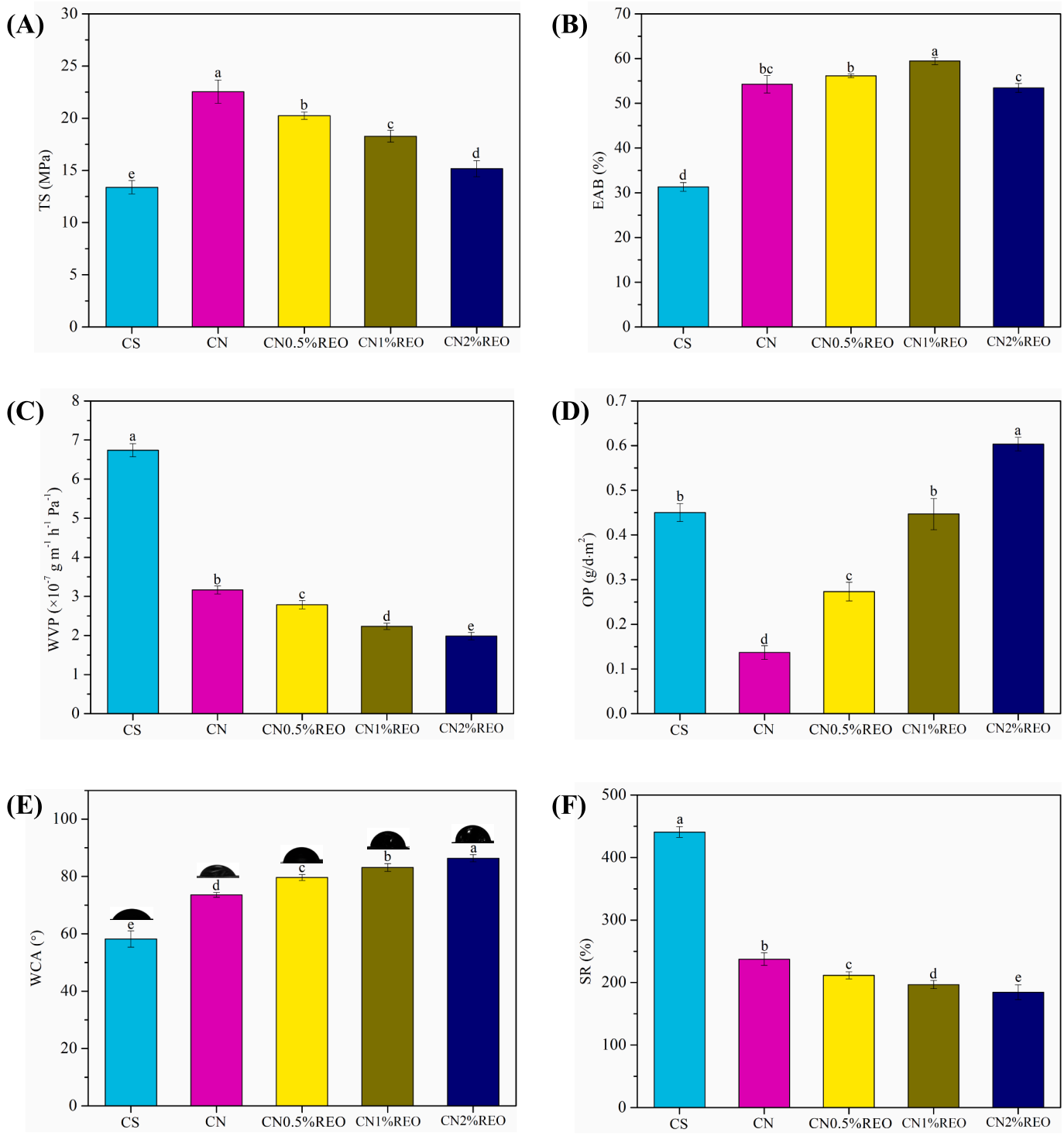

Fig. 5. TS (A), EAB (B), WVP (C), OP (D), WCA (E) and SR (F) of CS, CN, CN0.5 %REO, CN1%REO and CN2%REO. Different letters in the same column indicate significantly different ($p < 0.05$).

REO resulted in the progressive modification of the stress–strain profiles of composite films, indicating a significant change in the mechanical properties of the film. The TS of CS was the lowest, and the TS of CN was significantly increased after incorporation of the chitin nanofibers ($p < 0.05$). The addition of 5 wt% chitin nanofibers approximately doubled the TS of CS. Here, the chitin nanofibers acted as reinforcing agents for the chitosan-based films and generated higher TS values. Hug et al. (2012) found a similar phenomenon in which cellulose nanocrystals enhanced the TS of alginate-based films. The enhancement of TS could be attributed to the good interfacial interaction between chitin nanofibers and the chitosan matrix resulting from their similar polysaccharide structures. In addition, the TS enhancement was also related to electrostatic interactions and intermolecular hydrogen bonding between the negatively charged esterified chitin nanofibers and positively charged chitosan (Leite, Moreira, Mattoso, & Bras, 2021). However, with the incorporation of REO, the TS of the film decreased distinctly ($p < 0.05$). The mechanical properties of biopolymer films are usually regulated by the intermolecular forces and the network microstructure

of the film matrix. The changes in TS may be due to the structural discontinuity caused by the weakened intermolecular interaction after the addition of REO in the polymer-based film network. Wang et al. (2021) also found a similar phenomenon: the addition of bamboo leaf essential oil distinctly decreased the TS of corn starch-based films. It should be noted that although the TS of the composite film was decreased after the incorporation of REO, the TS of CN2%REO was still significantly higher than that of pure CS ($p < 0.05$). The reasons were due to the film matrix being reinforced by the chitin nanofibers, which diminished the effects of REO on the TS of films. The EAB value of CS was the lowest, and the EAB of the film was significantly enhanced after incorporation of the chitin nanofibers. This was related to the compact structure of the films and the strong interactions between the chitin nanofibers and the film matrix. With increasing REO content (0.5–1%), the EAB of the film was significantly increased. As a form of oil droplet, OPEO easily deformed and penetrated into the film matrix; thus, the microstructure of the film discontinuity was triggered by weak bonding between the polymer chains, which resulted in partial fracture of the film network but made the film more flexible; this was consistent with the results of our SEM analysis. Wang et al. (2021) also reported that when bamboo leaf volatile oil was incorporated into a starch film, the strong interactions between the polysaccharides in the starch-based film were replaced by weak interactions between the essential oil and the polysaccharides, making the structure of the starch film more flexible and leading to an increase in the EAB. However, as the REO content in the film reached 2%, the EAB of the film declined significantly ($p < 0.05$), which may be due to the excessive addition of essential oil and the destruction of the internal structure of the film. It is acceptable that the EAB of the biocomposite films was still higher than that of pure CS due to the presence of chitin nanofibers reinforcement.

3.5. WVP and OP

Fig. 5C shows the effect of chitin nanofibers and REO on the WVP of the chitosan-based films. CS had the highest WVP value of 6.74 ± 0.17. After incorporation of the chitin nanofibers, the WVP of the film was significantly reduced ($p < 0.05$). Moreover, only 5 wt% chitin nanofibers were incorporated, and the WVP was reduced by more than 50%. This was related to the strong interactions between the chitin nanofibers and the film matrix. After the chitin nanofibers were added, the film formed a dense microstructural network, which was beneficial to enhancing the water vapor barrier capacity. Previous studies have also found that cellulose nanofibers can decrease the WVP value of polymer films (Huq, et al., 2012; Jiang et al., 2021a). As the essential oil content was increased, the WVP value of chitosan-based films significantly decreased ($p < 0.05$), suggesting that the addition of hydrophobic substances can reduce the WVP of film. The reason was that the addition of hydrophobic essential oil to biopolymer films can increase the zigzag factor, making the path of water through the polymer films zigzag, hence reducing the WVP of the film (Wang, et al., 2021). Although there were microporous structures in the film containing the essential oil, these micropores increased the lengths of the tortuous paths allowing water vapor to pass through the film. Some water vapor blocked in the film may make the water vapor pass through the film more slowly, preventing the water vapor from passing through the film. Moreover, a previous study reported that essential oil can be uniformly dispersed in film, forming hydrophobic oil agglomerates that impair the mobility of water molecules in biopolymer film (Li et al., 2021).

The effects of the chitin nanofibers and REO on the OP of the chitosan-based films are shown in Fig. 5D. After the chitin nanofibers were added, the OP value of the film significantly ($p < 0.05$) decreased. This was because the chitin nanofibers formed a dense network structure through electrostatic interactions and intermolecular hydrogen bonding with the film matrix, which was beneficial for enhancing the barrier capacity of the films. Nevertheless, when the essential oil was incorporated, the OP value of the films was notably ($p < 0.05$) increased. The reason may be that the incorporation of essential oil increased the number of pores in the film, and with the increase in the amount of essential oil, the pore size gradually increased, which increased the opportunity for gas to penetrate the film.

3.6. WCA and SR

The water resistance of the chitosan-based active packaging is a crucial obstacle to application. The WCA value is used to reflect the water sensitivity of a film surface. Typically, films with WCA greater than 65° are hydrophobic, and<65° are hydrophilic (Li et al., 2021a). The WCA results for the chitosan-based composite films are displayed in Fig. 5E. CS had the lowest WCA ($58.20 \pm 2.85°$), consistent with its hydrophilic properties. After incorporation of the chitin nanofibers, the WCA of the chitosan film was significantly increased ($p < 0.05$), which indicated that the surface hydrophobicity of the chitosan film was improved. This is because the chitin nanofibers are hydrophobic, and increasing amounts of hydrophobic substances in the film increased the WCA. The chitin nanofibers formed hydrogen bonds with hydrophilic groups in the film matrix, which weakened the interactions between water and the hydrophilic groups in the films (Wang et al., 2023). The WCA for the chitosan-based composite films increased significantly with increasing amounts of REO added ($p < 0.05$). When the proportion of essential oil reached 2%, the WCA of the film was approximately 86°, indicating that the incorporation of REO enhanced the hydrophobicity of the film. Similarly, the addition of orange peel essential oil also enhanced the WCA of a chitosan/gelatin film (Li et al., 2021a). The results described above showed that the esterified chitin nanofibers and REO synergistically improved the hydrophobicity of the chitosan-based films.

The SR results for the chitosan-based composite films are displayed in Fig. 5F. Pure CS had the highest SR ($440.68 \pm 8.69\%$). After the chitin nanofibers were added, the SR of CS decreased significantly by approximately 200% ($p < 0.05$). The reason was that the strong intermolecular and electrostatic interactions between the esterified chitin nanofibers and chitosan limited water absorption by the film. With increases in the essential oil content, the SR of the composite films decreased significantly ($p < 0.05$). There were two main reasons for this: (i) the decreased SR was due to the increased hydrophobicity of the CN-REO films. The essential oil was hydrophobic, and the added REO increased the hydrophobicity of the films. (ii) The strong interactions between the essential oil and the film matrix reduced the swelling degree of the polymer chains in the interface region (Jiang et al., 2021c). Zhang et al. (2018) also reported that the SR of a chitosan composite film decreased significantly after addition of *Perilla frutescens* (L.) Britt. essential oil. These results showed that the esterified chitin nanofibers and REO synergistically reduced the SR of the chitosan-based films. The hydrophobicity of CN2%REO indicated that it has great potential for used in packaging foods with high water contents.

3.7. Antioxidant capacity of films

Antioxidant activity is an important aspect of the performance of active packaging. DPPH and ABTS scavenging tests were performed to determine the antioxidant capacity of the films. The DPPH and ABTS radical scavenging activity of the films are displayed in Fig. 6A-B. The ABTS and DPPH scavenging ratios for CS were the lowest, at $12.65 \pm 1.31\%$ and $19.52 \pm 0.74\%$, respectively, which suggested poor antioxidant activity for CS. Similar phenomena were reported in previous studies (Wang et al., 2023; Li et al., 2021a). Addition of the chitin nanofibers did not significantly improve the antioxidant capacity of the chitosan-based film (p greater than 0.05), which was due to the lack of antioxidant activity of chitin. Our previous study also showed that cellulose nanocrystals did not improve the antioxidant activity of zein films (Jiang et al., 2021a). With the incorporation of REO, the scavenging ratios of DPPH and ABTS of the films were notably enhanced ($p < 0.05$).

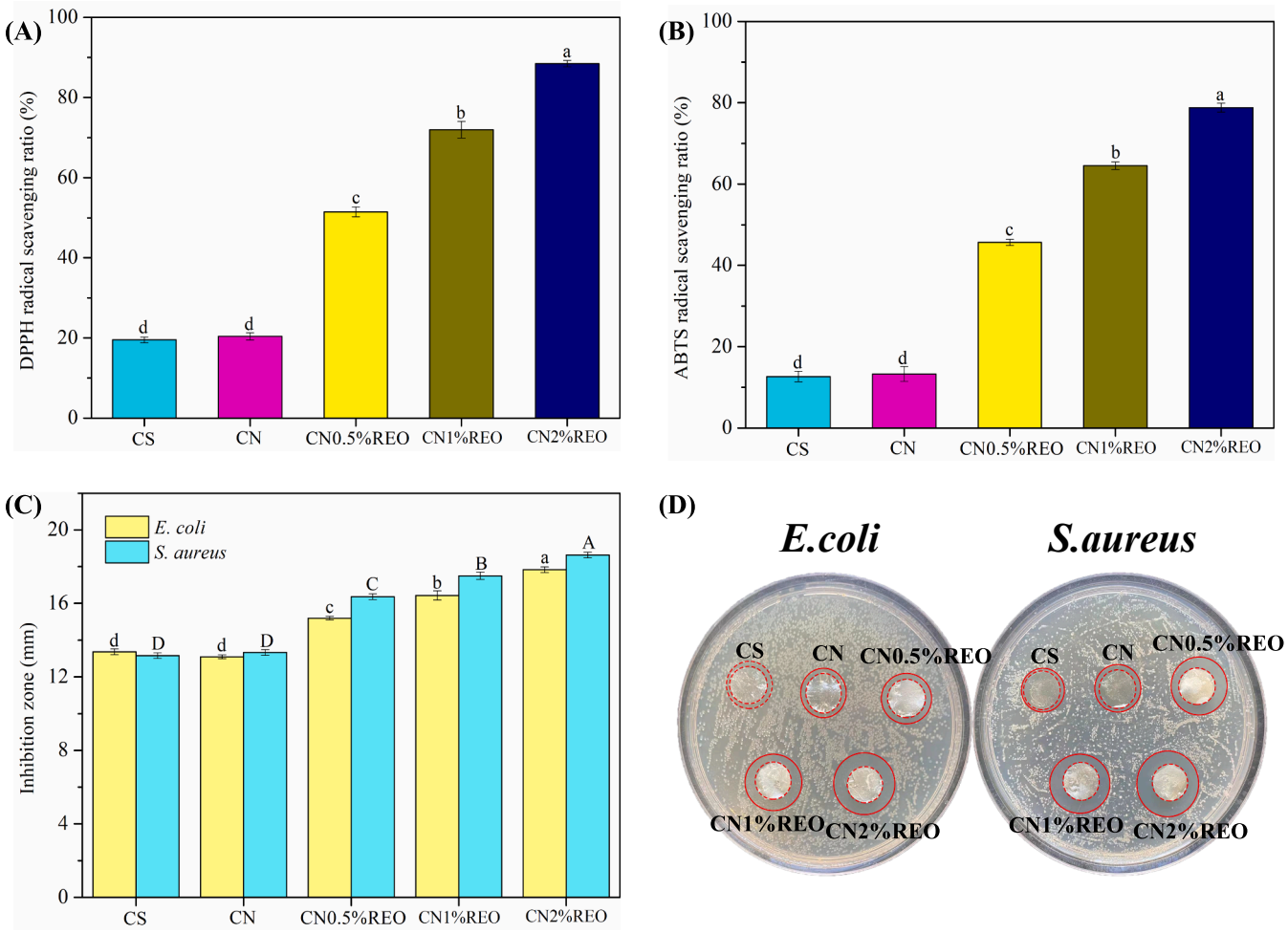

Fig. 6. DPPH radical scavenging activity (A), ABTS radical scavenging activity (B), antimicrobial activity (C) and the image of antimicrobial activity (D) of the films. Different letters in the same column indicate significantly different ($p < 0.05$).

When 2% REO was added, the DPPH and ABTS free radical scavenging reached 88.46 ± 0.79% and 78.81 ± 1.08%, respectively. These results indicated that the incorporation of REO significantly enhanced the antioxidant activity of the chitosan-based films. In general, essential oils are reported as an excellent sources of antioxidants and are widely used in cosmetics, medicines, food preservatives and in other fields (Pan, et al., 2023). The antioxidant activity of REO is attributed to antioxidant components such as polyphenols and flavonoids (Cendrowski et al., 2017b). The hydroxyl groups present in the phenolic compounds of the essential oils are typically attached to carbon atoms of the aromatic rings, which facilitates hydrogen atom donation to free radicals and thus impedes oxidation (Bhowmik, Agyei, & Ali, 2022). Donating hydrogen atoms (H) is useful to stop oxidative damage and chain reactions. A previous study also reported that essential oils could improve the antioxidant activity of biopolymer films (Li et al., 2021a).

3.8. Antimicrobial activity of films

The agar disk diffusion method was used with chitosan-based films containing chitin nanofibers and different concentrations (0, 0.5, 1 and 2%) of REO to verify their antimicrobial activity against *E. coli* and *S. aureus*. As shown in Fig. 6C, the incorporation of chitin nanofibers did not significantly improve the antibacterial activity of the film ($p > 0.05$). Previous studies reached the same conclusion (Wang et al., 2023). However, with increasing REO levels, the antimicrobial activity of chitosan-based films was gradually enhanced. Compared with that of pure CS, the incorporation of REO significantly ($p < 0.05$) increased the antibacterial capacity of the chitosan-based films. Digital photos showed that the films containing the essential oil had the best antibacterial activities, and the inhibition area increased significantly with increases in REO content (Fig. 6D). It has been reported that biopolymer films containing essential oils slowly release the volatile oils to the surrounding medium; the essential oils come into contact with the *S. aureus* and *E. coli*, which leads to bacteriostatic effects and inhibited microbial growth (Wang, et al., 2021). Thus, the antimicrobial activity of the composite films containing REO may have been provided by the REO. The hydrophobic nature of REO is responsible for attaching to and boring into the lipid components of the microbial cell membranes, thereby enhancing the permeability of the bacterial cell membranes (Bhowmik et al., 2022). Contact between the essential oils and the bacterial cell membranes inhibits the proliferation of both gram-positive and gram-negative bacteria. Antibacterial action has been associated with reduced membrane synthesis, loss of inorganic components, protein dysfunction, proton pump breakdown, inhibition of nucleic acid synthesis, and reduced ATP production (Bhowmik et al., 2022). The plasma membranes of bacterial cells allow easy penetration of ions and protons. Essential oils are therefore able to tamper with the protein and lipid layers of bacterial cells, thereby promoting coagulation of the cytoplasmic contents, loss of the intracellular components, disruption of the enzyme systems and reduced cell metabolism, which lead to bacterial cell death (Bhowmik et al., 2022). In addition, the antibacterial effects of essential oils may be due to the interaction of the active ingredients in essential oils with the permeability of cell membranes, resulting in the leakage of cell contents that are essential for microbial

survival. The main components of the REO included citronellol, geraniol, and eugenol, which have strong antibacterial activity. Notably, the CN-REO films exhibited greater inhibition of gram-positive bacteria (*S. aureus*) than gram-negative bacteria (*E. coli*); this was attributed to differences in the wall types of gram-negative and gram-positive bacteria. In gram-negative bacteria, an additional outer membrane around the cell wall limits the diffusion of hydrophobic compounds through the lipopolysaccharide layer, thus making them more resistant to antimicrobials (Saricaoglu and Turhan, 2020). Many studies have reached the conclusion that essential oils are less effective against gram-negative bacteria than against gram-positive bacteria (Wang et al., 2021). In summary, chitosan-based films containing REO show the potential for use in antibacterial food packaging materials designed to resist invasion of the food by microorganisms.

4. Conclusion

The present study developed a novel biocomposite film prepared from a range of sources, including renewable, eco-friendly polymers (chitosan and chitin nanofibers) and natural REO. The structures of the composite biofilms were characterized by XRD, SEM, FT-IR and TGA. These results showed that the chitin nanofibers and REO had significant impacts on the chemical structure and morphology of the chitosan-based composite films. The esterified negatively charged chitin nanofibers can improve the mechanical and barrier properties of the biofilms by forming electrostatic interactions and intermolecular hydrogen bonds with the film matrix. The chitosan-based films containing REO resisted UV radiation, especially CN2%REO, which exhibited the best UV blocking ability. The incorporation of REO significantly reduced the transparency and glossiness of the chitosan-based films, which can be used in packaging food that is sensitive to light. Moreover, the added chitin nanofibers and REO reduced the water vapor permeability of the film, which prevented water exchange between the external environment and the food and thus has the potential to extend the shelf life of foods. The incorporated REO significantly improved the water resistances of the chitosan composite films, especially when the highest proportion of essential oil was used (CN2%REO). In addition, the chitin nanofibers had no significant effect on the antioxidant and antibacterial capacity of the chitosan-based biofilms. However, the incorporation of essential oil significantly enhanced the bioactivity (antibacterial and antioxidant activity) of chitosan-based films, and CN2%REO had the strongest antibacterial and antioxidant activity. CN2%REO exhibited the most potent biological activity, so it is the optimal candidate for industrial development as a multifunctional food packaging material. Moreover, our results suggested that CN2%REO has good physical properties and the best antibacterial and antioxidant activities among the films studied; it has great potential for use in food packaging designed to extend food shelf life. However, it is also important to consider the impacts of the CN-REO films (used as food packaging materials) on food storage quality and shelf life and to evaluate their practicability and effectiveness, which will be the focus of our future research.

CRediT authorship contribution statement

Yingzhu Liu: Conceptualization, Methodology, Data curation, Investigation, Validation, Writing – original draft, Formal analysis. **Rongxu Liu:** Investigation, Software, Writing – review & editing. **Jingbo Shi:** Investigation, Software. **Rui Zhang:** Visualization. **Hongjie Tang:** Data curation. **Cancan Xie:** Investigation. **Fenghui Wang:** Software. **Jianchun Han:** Conceptualization, Supervision, Funding acquisition, Writing – review & editing. **Longwei Jiang:** Writing – review & editing, Project administration, Funding acquisition, Methodology, Supervision.

Declaration of Competing Interest

The authors declare that they have no known competing financial interests or personal relationships that could have appeared to influence the work reported in this paper.

Data availability

The authors do not have permission to share data.

Acknowledgements

This work was financially supported by the Research Funds of Heilongjiang Scientific Research Institutes (CZKYF2022-1-A001), the China Postdoctoral Science Foundation (2022MD723756) and Youth Project of Heilongjiang Provincial Natural Science Foundation (YQ2021C014).

Appendix A. Supplementary data

Supplementary data to this article can be found online at https://doi.org/10.1016/j.fochx.2023.100714.

References

Alizadeh-Sani, M., Rhim, J.-W., Azizi-Lalabadi, M., Hemmati-Dinarvand, M., & Ehsani, A. (2020). Preparation and characterization of functional sodium caseinate/guar gum/TiO_2/cumin essential oil composite film. *International Journal of Biological Macromolecules, 145*, 835–844.

Bakshi, P. S., Selvakumar, D., Kadirvelu, K., & Kumar, N. S. (2020). Chitosan as an environment friendly biomaterial – a review on recent modifications and applications. *International Journal of Biological Macromolecules, 150*, 1072–1083.

Bhowmik, S., Agyei, D., & Ali, A. (2022). Bioactive chitosan and essential oils in sustainable active food packaging: Recent trends, mechanisms, and applications. *Food Packaging and Shelf Life, 34*, Article 100962.

Cebi, N. (2021). Quantification of the Geranium Essential Oil, Palmarosa Essential Oil and Phenylethyl Alcohol in Rosa damascena Essential Oil Using ATR-FTIR Spectroscopy Combined with Chemometrics. *Foods, 10*(8), 1848.

Cebi, N., Arici, M., & Sagdic, O. (2021). The famous Turkish rose essential oil: Characterization and authenticity monitoring by FTIR, Raman and GC-MS techniques combined with chemometrics. *Food Chemistry, 354*, Article 129495.

Cendrowski, A., Scibisz, I., Kieliszek, M., Kolniak-Ostek, J., & Mitek, M. (2017a). UPLC-PDA-Q/TOF-MS Profile of Polyphenolic Compounds of Liqueurs from Rose Petals (*Rosa rugosa*). *Molecules, 22*(11), 1832.

Cendrowski, A., Scibisz, I., Mitek, M., Kieliszek, M., & Kolniak-Ostek, J. (2017b). Profile of the Phenolic Compounds of Rosa rugosa Petals. *Journal of Food Quality, 7941347*.

Cendrowski, A., Scibisz, I., Mitek, M., & Kieliszek, M. (2018). Influence of harvest seasons on the chemical composition and antioxidant activity in Rosa rugosa petals. *Agrochimica, 62*(2), 157–165.

Chen, Z., Wen, J., Huang, S., Sun, Y., Liu, X., Chen, L., … Zhao, P. (2023). Highly TVB-N sensitive film with CMS as the 'bridge' via electrostatic interaction and hydrogen bond self-assembly for monitoring food freshness in intelligent packaging. *Talanta, 252*, Article 123881.

Choo, K. W., Lin, M., & Mustapha, A. (2021). Chitosan/acetylated starch composite films incorporated with essential oils: Physiochemical and antimicrobial properties. *Food Bioscience, 43*, Article 101287.

Chu, Y., Cheng, W., Feng, X., Gao, C., Wu, D., Meng, L., … Tang, X. (2020). Fabrication, structure and properties of pullulan-based active films incorporated with ultrasound-assisted cinnamon essential oil nanoemulsions. *Food Packaging and Shelf Life, 25*, Article 100547.

Danopoulos, E., Twiddy, M., West, R., & Rotchell, J. M. (2022). A rapid review and meta-regression analyses of the toxicological impacts of microplastic exposure in human cells. *Journal of Hazardous Materials, 427*, Article 127861.

de Souza, A., dos Santos, N., da Silva Torin, R., & dos Santos Rosa, D. (2020). Synergic antimicrobial properties of Carvacrol essential oil and montmorillonite in biodegradable starch films. *International Journal of Biological Macromolecules, 164*, 1737–1747.

Ding, F. Y., Deng, H. B., Du, Y. M., Shi, X. W., & Wang, Q. (2014). Emerging chitin and chitosan nanofibrous materials for biomedical applications. *Nanoscale, 6*(16), 9477–9493.

Flórez, M., Cazón, P., & Vázquez, M. (2022). Active packaging film of chitosan and Santalum album essential oil: Characterization and application as butter sachet to retard lipid oxidation. *Food Packaging and Shelf Life, 34*, Article 100938.

Geng, Y., Xue, H., Zhang, Z., Panayi, A. C., Knoedler, S., Zhou, W., … Liu, G. (2023). Recent advances in carboxymethyl chitosan-based materials for biomedical applications. *Carbohydrate Polymers, 305*, Article 120555.

Hafsa, J., Smach, M.a., Ben Khedher, M. R., Charfeddine, B., Limem, K., Majdoub, H., & Rouatbi, S. (2016). Physical, antioxidant and antimicrobial properties of chitosan films containing Eucalyptus globulus essential oil. *LWT - Food Science and Technology, 68*, 356–364.

Han, Y., Lian, F., Xiao, Z., Gu, S., Cao, X., Wang, Z., … Xing, B. (2022). Potential toxicity of nanoplastics to fish and aquatic invertebrates: Current understanding, mechanistic interpretation, and meta-analysis. *Journal of Hazardous Materials, 427*, Article 127870.

Huq, T., Salmieri, S., Khan, A., Khan, R. A., Le Tien, C., Riedl, B., … Lacroix, M. (2012). Nanocrystalline cellulose (NCC) reinforced alginate based biodegradable nanocomposite film. *Carbohydrate Polymers, 90*(4), 1757–1763.

Jafari, H., Pirouzifard, M., Khaledabad, M. A., & Almasi, H. (2016). Effect of chitin nanofiber on the morphological and physical properties of chitosan/silver nanoparticle bionanocomposite films. *International Journal of Biological Macromolecules, 92*, 461–466.

Jardine, A., & Sayed, S. (2018). Valorisation of chitinous biomass for antimicrobial applications. *Pure and Applied Chemistry, 90*(2), 293–304.

Jiang, L., Han, Y., Meng, X., Xiao, Y., & Zhang, H. (2021a). Cellulose Nanocrystals Reinforced Zein/Catechin/β-Cyclodextrin Inclusion Complex Nanoparticles Nanocomposite Film for Active Food Packaging. *Polymers (Basel), 13*(16), 2759.

Jiang, L., Jia, F., Han, Y., Meng, X., Xiao, Y., & Bai, S. (2021b). Development and characterization of zein edible films incorporated with catechin/β-cyclodextrin inclusion complex nanoparticles. *Carbohydrate Polymers, 261*, Article 117877.

Jiang, L., Luo, Z., Liu, H., Wang, F., Li, H., Gao, H., … Zhang, H. (2021c). Preparation and Characterization of Chitosan Films Containing Lychee (*Litchi chinensis* Sonn.) Pericarp Powder and Their Application as Active Food Packaging. *Foods, 10*(11), 2834.

Jiang, L., Liu, F., Wang, F., Zhang, H., & Kang, M. (2022a). Development and characterization of zein-based active packaging films containing catechin loaded β-cyclodextrin metal-organic frameworks. *Food Packaging and Shelf Life, 31*, Article 100810.

Jiang, L., Wang, F., Xie, X., Xie, C., Li, A., Xia, N., … Zhang, H. (2022b). Development and characterization of chitosan/guar gum active packaging containing walnut green husk extract and its application on fresh-cut apple preservation. *International Journal of Biological Macromolecules, 209*, 1307–1318.

Leite, L. S. F., Moreira, F. K. V., Mattoso, L. H. C., & Bras, J. (2021). Electrostatic interactions regulate the physical properties of gelatin-cellulose nanocrystals nanocomposite films intended for biodegradable packaging. *Food Hydrocolloids, 113*, Article 106424.

Li, Y., Tang, C., & He, Q. (2021a). Effect of orange (*Citrus sinensis* L.) peel essential oil on characteristics of blend films based on chitosan and fish skin gelatin. *Food Bioscience, 41*, Article 100927.

Li, T., Xia, N., Xu, L., Zhang, H., Zhang, H., Chi, Y., … Li, H. (2021b). Preparation, characterization and application of SPI-based blend film with antioxidant activity. *Food Packaging and Shelf Life, 27*, Article 100614.

Maciąg, A., & Kalemba, D. (2015). Composition of rugosa rose (*Rosa rugosa* thunb.) hydrolate according to the time of distillation. *Phytochemistry Letters, 11*, 373–377.

Pasquier, E., Mattos, B. D., Koivula, H., Khakalo, A., Belgacem, M. N., Rojas, O. J., … Bras, J. (2022). Multilayers of Renewable Nanostructured Materials with High Oxygen and Water Vapor Barriers for Food Packaging. *ACS Applied Materials & Interfaces*.

Ragusa, A., Notarstefano, V., Svelato, A., Belloni, A., Gioacchini, G., Blondeel, C., … Giorgini, E. (2022). Raman Microspectroscopy Detection and Characterisation of Microplastics in Human Breastmilk. *Polymers (Basel), 14*(13), 2700.

Saricaoglu, F. T., & Turhan, S. (2020). Physicochemical, antioxidant and antimicrobial properties of mechanically deboned chicken meat protein films enriched with various essential oils. *Food Packaging and Shelf Life, 25*.

Shahzadi, K., Wu, L., Ge, X., Zhao, F., Li, H., Pang, S., … Mu, X. (2016). Preparation and characterization of bio-based hybrid film containing chitosan and silver nanowires. *Carbohydrate Polymers, 137*, 732–738.

Tang, Y., Zhang, X., Zhao, R., Guo, D., & Zhang, J. (2018). Preparation and properties of chitosan/guar gum/nanocrystalline cellulose nanocomposite films. *Carbohydrate Polymers, 197*, 128–136.

Wang, B., Yan, S., Gao, W., Kang, X., Yu, B., Liu, P., … Abd El-Aty, A. (2021). Antibacterial activity, optical, and functional properties of corn starch-based films impregnated with bamboo leaf volatile oil. *Food Chemistry, 357*, Article 129743.

Wang, Q., Yan, X., Chang, Y., Ren, L., & Zhou, J. (2018). Fabrication and characterization of chitin nanofibers through esterification and ultrasound treatment. *Carbohydrate Polymers, 180*, 81–87.

Wang, Y., Wang, X., Hu, G., Al-Romaima, A., Liu, X., Bai, X., … Qiu, M. (2022). Effect of green coffee oil as a natural active emulsifying agent on the properties of corn starch-based films. *LWT - Food Science and Technology, 170*, Article 114087.

Wang, F., Xie, C., Tang, H., Hao, W., Wu, J., Sun, Y., … Jiang, L. (2023). Development, characterization and application of intelligent/active packaging of chitosan/chitin nanofibers films containing eggplant anthocyanins. *Food Hydrocolloids, 139*, Article 108496.

Yin, K., Wang, Y., Zhao, H., Wang, D., Guo, M., Mu, M., … Xing, M. (2021). A comparative review of microplastics and nanoplastics: Toxicity hazards on digestive, reproductive and nervous system. *Science of The Total Environment, 774*, Article 145758.

Zhang, N., Bi, F., Xu, F., Yong, H., Bao, Y., Jin, C., … Liu, J. (2020). Structure and functional properties of active packaging films prepared by incorporating different flavonols into chitosan based matrix. *International Journal of Biological Macromolecules, 165*, 625–634.

Zhang, Z.-J., Li, N., Li, H.-Z., Li, X.-J., Cao, J.-M., Zhang, G.-P., … He, D. (2018). Preparation and characterization of biocomposite chitosan film containing *Perilla frutescens* (L.) Britt. essential oil. *Industrial Crops and Products, 112*, 660–667.